

**Molecular-Level Details of
Morphology-Dependent Exciton Migration in
Poly(3-hexylthiophene) Nanostructures
(Supporting Information)**

Patrick C. Tapping, Scott N. Clifton, Kyra N. Schwarz,^a Tak W. Kee, and
David M. Huang*

Department of Chemistry, The University of Adelaide, South Australia 5005, Australia

E-mail: david.huang@adelaide.edu.au

Phone: +61-8-8313-5580

^aCurrent address: School of Chemistry, University of Melbourne, Parkville, VIC, 3010 Australia

*To whom correspondence should be addressed

Model Parametrization

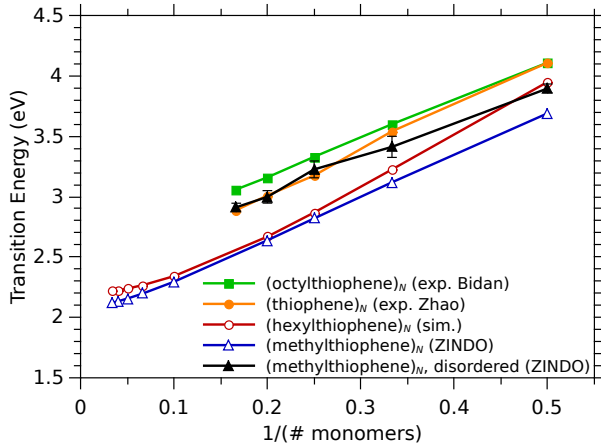


Figure S1: Transition energies of thiophene oligomers as a function of the inverse number of monomer units. Transition energies of planar methylthiophene oligomers were computed using the ZINDO/S method (blue open triangles). The values for the sum of the nearest-neighbor exciton transfer integral components, $(J^{\text{SE}} + J^{\text{DD}})$, and nominal on-site excitation energy, E_0 , were then selected by fitting the predicted LEGS energies of planar coarse-grained structures (red open circles) to the slope and offset respectively for oligomers of length 5–30 units. Experimental data for octylthiophene oligomers in chloroform¹ (orange filled circles) and thiophene oligomers in benzene² (green filled squares) are included for comparison. The experimental oligomers are not expected to be perfectly planar and possess some degree of disorder. For comparison, disordered methylthiophene oligomers were constructed using dihedral angles between the thiophene units selected randomly from the expected Boltzmann distribution at 298 K³ and their transition energies computed using the ZINDO/S method (black filled triangles). For oligomers of N units, $3(N - 1)$ different structures were generated. Error bars are 2 standard errors.

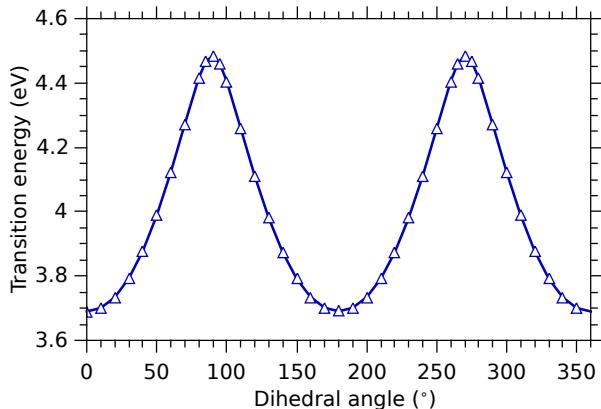


Figure S2: Transition energy of a methylthiophene dimer as a function of the dihedral angle between the thiophene units, computed using the ZINDO/S method. The through-bond superexchange contribution of the nearest neighbor exciton transfer integral, J^{SE} , is determined from the difference in transition energy between the planar and orthogonal orientations.

Time-Resolved Fluorescence

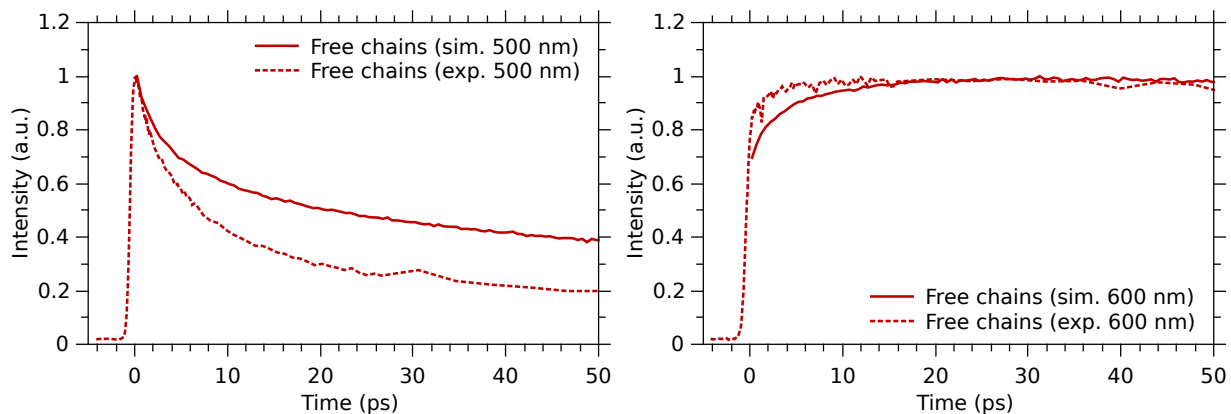


Figure S3: Simulated and experimental time-resolved fluorescence of P3HT chains in solution showing the dynamic red-shift of the fluorescence is captured in the simulation. 500 nm is on the blue side of the emission peak, and 600 nm is on the red side. The differing shape of the traces indicates the peak undergoes a red-shift over several picoseconds.

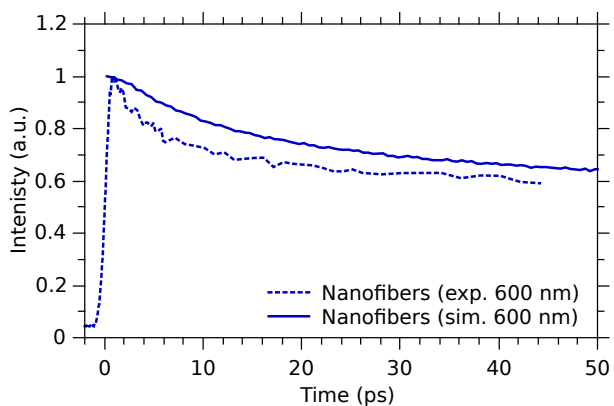


Figure S4: Simulated and experimental time-resolved fluorescence of P3HT nanofibers. 600 nm is approximately at the center of the emission peak.

Exciton Migration Preference

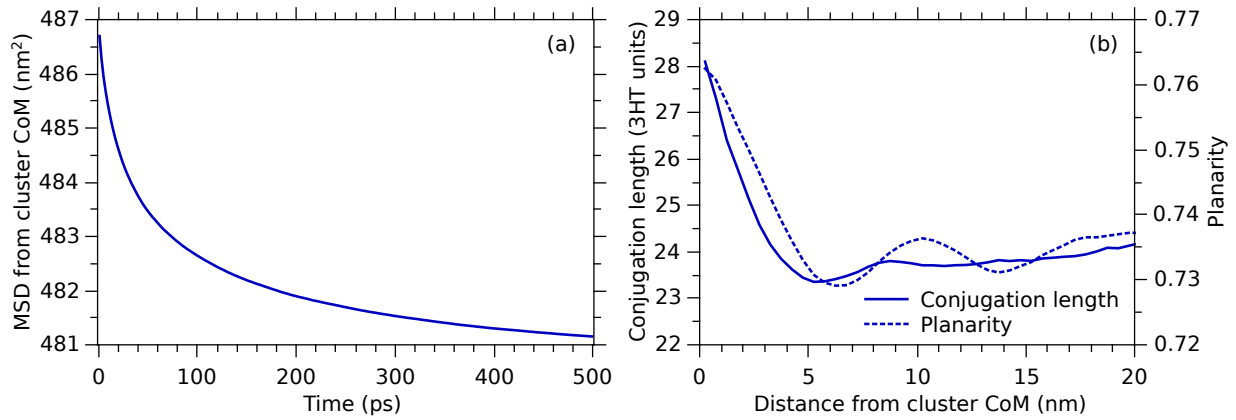


Figure S5: (a) Mean squared displacement of the exciton relative to the nanofiber cluster's center of mass. (b) Mean chromophore length and planarity of the polymer relative to the distance from the center of mass of the nanofiber cluster. Planarity is defined as $\frac{3}{2} \cos^2 \phi - \frac{1}{2}$, where ϕ is the dihedral angle between monomer units.

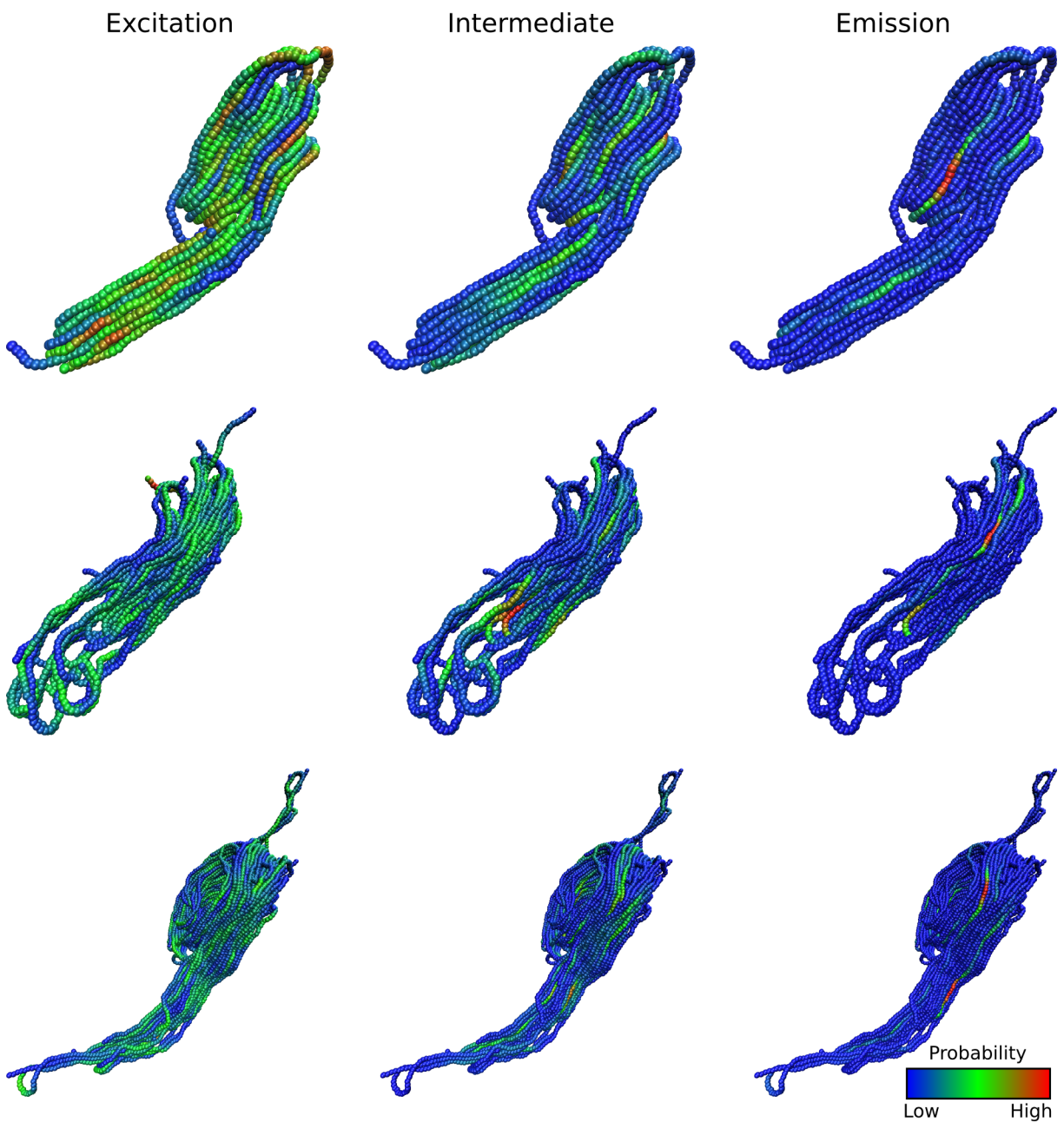


Figure S6: Probability heat maps of excitation, intermediate exciton visit, and emission events on P3HT nanofiber aggregates. A large proportion of chromophores act as absorbing sites, while only a small number are sites of high intensity emission. These low-energy “trap” sites are often located at the core, rather than the surface of the aggregate.

Fluorescence Depolarization Rates

Single-exponential decay fits of the form $A = A_0 + B \exp(-t/\tau)$ were made to the simulated and experimental fluorescence anisotropy data over the first 25 ps to extract the depolarization time constant, τ . The exciton diffusion coefficient, D_t , was obtained by a linear fit to the exciton mean squared displacement plot over the first 25 ps. The quantity $1/\sqrt{\tau D_t}$ provides a measure of the degree of fluorescence depolarization per unit distance travelled by the exciton and gives an indication of the rate of fluorescence depolarization relative to that of exciton diffusion. The values shown in Table S1 indicate that the rate of depolarization is approximately equal for the free chains and nanofibers. (Note that the different appearance of the anisotropy traces is therefore primarily due to the differing amplitude factors, B .) However, the nanofibers show a significantly faster exciton diffusion rate. As a result, the exciton in nanofibers moves on average 40% further than that in free chains for the same amount of fluorescence depolarization.

Table S1: Comparison of fluorescence depolarization and exciton diffusion rates over the period of $t = 0$ to $t = 25$ ps.

System	τ (ps)	D_t (nm ² ps ⁻¹)	$1/\sqrt{\tau D_t}$ (nm ⁻¹)
Free chains	6.6	0.45	0.58
Nanofibers (hairpins)	7.1	0.77	0.43
Nanofibers (helices)	7.0	0.77	0.43
Free chains (exp.)	1.5	–	–
Nanofibers (exp.)	2.0	–	–

References

- (1) Bidan, G.; De Nicola, A.; Enée, V.; Guillerez, S. Synthesis and UV–Visible Properties of Soluble Regioregular Oligo(3-octylthiophenes), Monomer to Hexamer. *Chem. Mater.* **1998**, *10*, 1052–1058.
- (2) Zhao, M.-T.; Singh, B. P.; Prasad, P. N. A Systematic Study of Polarizability and Microscopic Third-Order Optical Nonlinearity in Thiophene Oligomers. *J. Chem. Phys.* **1988**, *89*, 5535–5541.
- (3) Schwarz, K. N.; Kee, T. W.; Huang, D. M. Coarse-Grained Simulations of the Solution-Phase Self-Assembly of Poly(3-hexylthiophene) Nanostructures. *Nanoscale* **2013**, *5*, 2017–2027.